ISSN Number: 2454-2024(Online)

International Journal of Technical Research & Science

DEVELOPMENT OF INTELLIGENT CONTROL STRATEGY FOR POWER QUALITY IMPROVEMENT OF HYBRID RES

Sachin Sharma, Raunak Jangid, Kapil Parikh

E-Mail Id: sachinsadhotra@gmail.com

Department of Electrical Engineering, SITE Nathdwara, Rajasthan, India

Abstract- The major problem in renewable energy system is that the variation in power generation from time to time because of the intermittent nature of the renewable sources. In this paper presents the Artificial Neural Network (ANN) based intelligent control strategy for hybrid standalone microgrid system for varying wind, varying solar irradiation, varying load and symmetrical and asymmetrical fault conditions is presented. A dynamic model of hybrid standalone microgrid consisting wind and solar PV renewable sources with maximum power point tracking control algorithm is developed in MATLAB/Simulink software. A solar PV panel, wind energy conversion system and dynamic model of hybrid energy storage consisting Lithium-ion batteries (Li-Ion) and supercapacitor is connected with the DC Bus. The DC link is connected through the power electronic interfacing circuit and converters connected to a source for a diverse electricity generation. The main objective of this thesis is to improve the power quality of the hybrid microgrid system by solving the voltage sag and swell problem and reduce total harmonics distortion occurring due to various symmetrical and asymmetrical condition. The simulation studies have been carried out to determine system performance with different scenarios of the sources such as typical solar radiation, temperature, wind, battery and supercapacitor charge or discharge conditions The proposed strategy gives better performance characteristics and reduces the harmonics of the system compared to the conventional solution.

Keywords: PV, WECS, Battery, ANN, Standalone Hybrid System.

1. INTRODUCTION

Due to the acute depletion of fossil fuel and atmosphere pollution, people are now fascinated with Renewable energy sources like PV, wind, hydro, etc. Solar and wind energy resources are affluently available all over the world. For the fluctuating nature of renewable energy resources, power generation from renewable energy systems is intermittent. These conditions inspired to combine two or more energy sources with the storage system to make Hybrid Renewable Energy System. A remote hybrid system gives a greater efficiency with a low cost of energy production, compared to the system with a single source. It is essential to take care of changes in the generated power which is varying from time to time. In literature, various types of HRES are introduced which are working in grid-connected or stand-alone mode. HRES system energy management is completed by using a PI controller. It is done by controlling a buck-boost bi-directional converter for battery charging and discharging. A current control strategy for power balance is introduced by the PI controller. The conventional controller strategy depends on mathematical modeling of the system. Hybrid systems are one effective solution for electrical energy generation, specifically for remote sites or for a micro-generation unit linked to a weak AC grid. The hybrid systems combine several conventional or renewable energy sources interconnected through a DC bus. For an isolated area, the association of electro-chemical storage with the hybrid system allows eliminating the diesel generator. In this condition, we describe a hybrid generation system acquired via combining PV and wind turbines with storage batteries to overcome periods of scant generation and for the system control. Various topologies are available for hybrid systems, depend on the interface converters amid sources and the interconnection technique. This system topology the interconnection of the sources with maximum energy transfer the investigation of energy losses involves power conditioning converters, optimal control and energy management. The present work aims to the idea of the hybrid system configuration, dynamic modeling, energy management and control strategies. The author proposes and investigates an efficient control strategy for energy management of standalone hybrid solar-wind system for different operating conditions. Due to the uninterrupted demand for energy, batteries backups are used in the hybrid system. So, the suggested system is efficient for working under variable weather and load conditions.

2. DESCRIPTION OF PROPOSED CONFIGURATION AND MODELING OF THE HRES

The proposed standalone hybrid microgrid system is developed along with the novel control strategy for power quality improvement features. The Microgrid consists a 9.8 Kw Photovoltaic (PV) system with Perturb and observe (P & O) MPPT algorithm to assure maximum power from PV panel and a 6.3Kw permanent magnet synchronous generator (PMSG) based wind energy conversion system (WECS) with optimum torque (OT) control maximum power point tracking (MPPT) to extract maximum power from wind. The hybrid energy storage system

(HESS) is connected to common DC bus to deliver power during emergency condition or to supply constant load power during variable load condition. The HESS configuration is developed consisting lithium-ion (Li-Ion) batteries and supercapacitor. A fully controlled AC/DC bridge rectifier is used to extract maximum power form the wind turbine. The gate pulse for the converter is generated by the optimum torque based MMPT technique. A DC/DC converter is used for the PV system and the gate pulse for the converter is developed by the P & O MPPT algorithm. Fig. 2.1 shows the block diagram of Developed Intelligent Control Strategy for Power Quality Improvement of Hybrid RES.

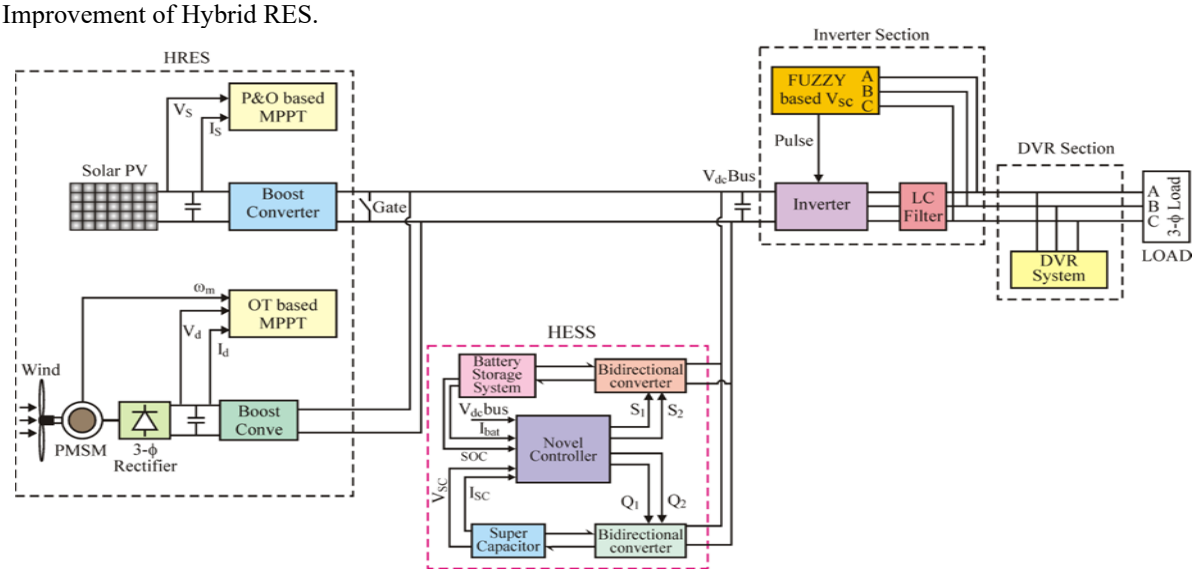

Fig. 2.1 Block diagram of Developed Intelligent Control Strategy for Power Quality Improvement of Hybrid RES

The power from the battery and supercapacitor can flow in the both directions, therefore two bi-directional DC/DC converter is implemented for controlling the power from both energy sources, these bi-directional converters are directly connected to the 640 V DC bus. When the wind and solar power is sufficient and the generated power exceeds the power demanded by the load then first the battery is charged.

3. PV SYSTEM MODELING

The equivalent circuit of a PV cell is shown in Fig. 3.1. The current source I_{ph} represents the cell photocurrent. R_{sh} and R_s are the intrinsic shunt and series resistances of the cell, respectively. Usually the value of R_{sh} is very large and that of R_s is very small, hence they may be neglected to simplify the analysis. Practically, PV cells are grouped in larger units called PV modules and these modules are connected in series or parallel to create PV arrays which are used to generate electricity in PV generation systems. The equivalent circuit for PV array is shown in Fig. 3.1.

The voltage–current characteristic equation of a solar cell is provided:

Module photo-current I_{ph}: $I_{ph} = [I_{SC} + K_i(T - 298)] * I_r/1000$

Here: I_{ph}: photo-current (A), I_{sc}: short circuit current (A), K_i: short-circuit current of cell at 25 °C and 1000 W/m^2, T: operating temperature (K), I_r: solar irradiation (W/m2).

Module reverse saturation current I_{rs}: $I_{rs} = I_{sc}/[\exp(qV_{oc}/N_S knT) - 1]$

Here: q: electron charge = 1.6 × 10−19C, V_{oc}: open circuit voltage (V), Ns: number of cells connected in series, n: the ideality factor of the diode, k: Boltzmann's constant, = 1.3805 × 10−23 J/K.

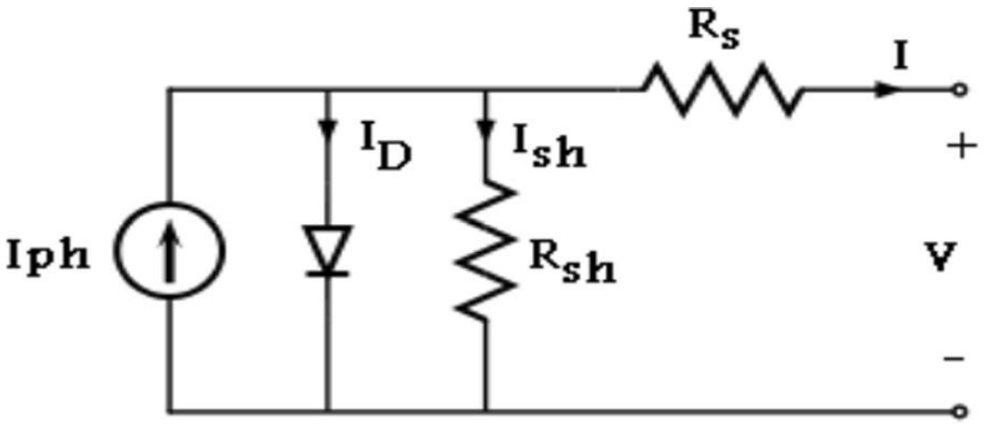

Fig. 3.1 PV Cell Equivalent Circuit

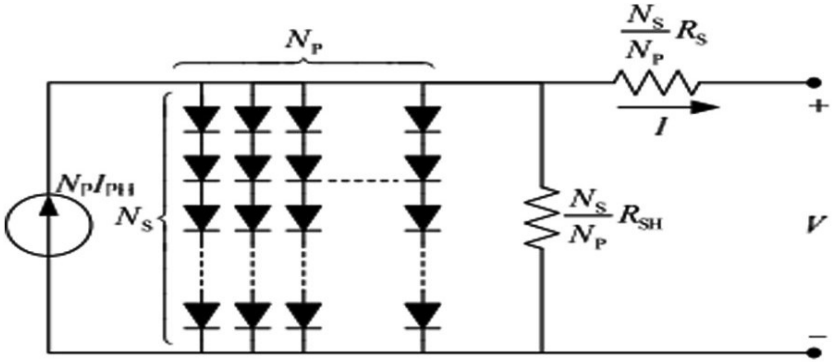

Fig. 3.2 Equivalent Circuit of Solar Array

The module saturation current I_0 varies with the cell temperature, which is given by:

$$I_0 = I_{rs}\left[\frac{T}{T_r}\right]^3 \exp\left[\frac{q \times E_{g0}}{nk}\left(\frac{1}{T} - \frac{1}{T_r}\right)\right] \quad (1)$$

Here: T_r: nominal temperature = 298.15 K, E_{g0}: band gap energy of the semiconductor = 1.1 eV The current output of PV module is:

$$I = N_P \times I_{ph} - N_P \times I_0 \times \left[\exp\left(\frac{V/N_S + I \times R_S/N_P}{n \times V_t}\right) - 1\right] - I_{sh} \quad (2)$$

$$\text{With } V_t = \frac{k \times T}{q} \text{ and } I_{sh} = \frac{V \times N_P/N_S + I \times R_S}{R_{sh}}$$

Here: Np: number of PV modules connected in parallel, R_s: series resistance (Ω), R_{sh}: shunt resistance (Ω), V_t: diode thermal voltage (V).

Table-3.1 Electrical Characteristics Data of Sun Power SPR-305E-WHT-U Module

Name	Sun Power SPR-305E-WHT-U
Rated power (V_{mp})	305.226 W
Voltage at maximum power (V_{mp})	54.7 V
Current at maximum power (I_{mp})	5.58 A
Open circuit voltage (V_{OC})	64.2 V
Short circuit current (I_{SC})	5.96 A
Total Series-connected modules per string	11
Total Parallel strings	3
Maximum system voltage	700 V
Range of operation temperature	−40 °C to 80 °C

4. WIND SYSTEM MODELING

The aim of the torque controller is to optimize the efficiency of capturing wind energy in a wide range of wind velocities, which retains the power generated by the machine as the optimal expressed value. It can be seen from the block diagram shown in Fig. 4.1. For any wind speed, the MPPT tool impose a torque reference accomplished of extracting maximum power. The curve T_{opt} is expressed by:

$$T_{opt} = K_{opt} * \omega_{opt}^2 \quad (3)$$

Where

$$K_{opt} = 0.5 * \rho A * \left(\frac{r_m}{\lambda_{opt}}\right)^3 * C_{P-max} \quad (4)$$

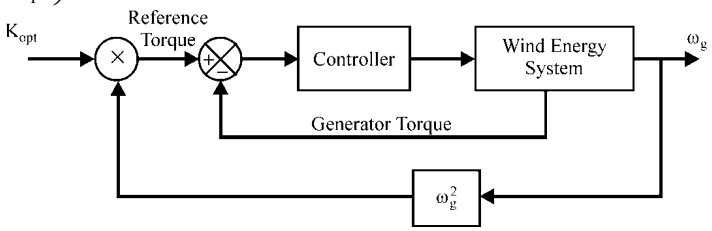

Fig. 4.1 Block Diagram of Optimal Torque Control MPPT Method

The PMSG model is presented in figure. This dynamic model assumes no saturation, a sinusoidal back e.m.f. and negligible eddy current and hysteresis losses. It takes into account the iron losses and the dynamic equations for the PMSG currents are:

$$\frac{di_{md}}{dt} = \frac{1}{L_d}(v_d - R_{st}i_d + \omega L_q i_{mq}), \quad (5)$$

$$\frac{di_{mq}}{dt} = \frac{1}{L_d}(v_q - R_{st}i_q + \omega L_q i_{md} - \omega \psi_{PM}), \quad (6)$$

$$i_d = \frac{1}{R_c}(L_d \frac{di_{md}}{dt} - \omega L_q i_{mq} + R_c i_{md}), \quad (7)$$

$$i_q = \frac{1}{R_c}(L_q \frac{di_{mq}}{dt} + \omega L_d i_{md} + \omega \psi_{PM} + R_c i_{mq}), \quad (8)$$

$$i_{cd} = i_d - i_{md}, \quad (9)$$

$$i_{cq} = i_q - i_{mq}, \quad (10)$$

where i_d, i_q are the d_q axes currents, V'_d, V_q are the d_q axes voltages, i'_{cd}, i_{cq} are the d_q axes iron losses currents, i_{md}, i_{mq} are the d_q axes magnetizing currents, L_d, L_q are the d_q axes inductances, If/PM is the mutual flux due to magnets, OJ is the fundamental frequency of the stator currents, R_c is the iron losses resistance and R_{st} is the stator resistance.

The electromagnetic torque equation of the PMSG is: $T_e = \frac{2}{3} p[\psi_{PM} i_{mq} + (L_d - L_q) i_{md} i_{mq}]$ (11)

where p is the number of pole pairs

5. MODELING OF BATTERIES

The Battery block implements a basic dynamic model parameterized to be best common types of rechargeable batteries.

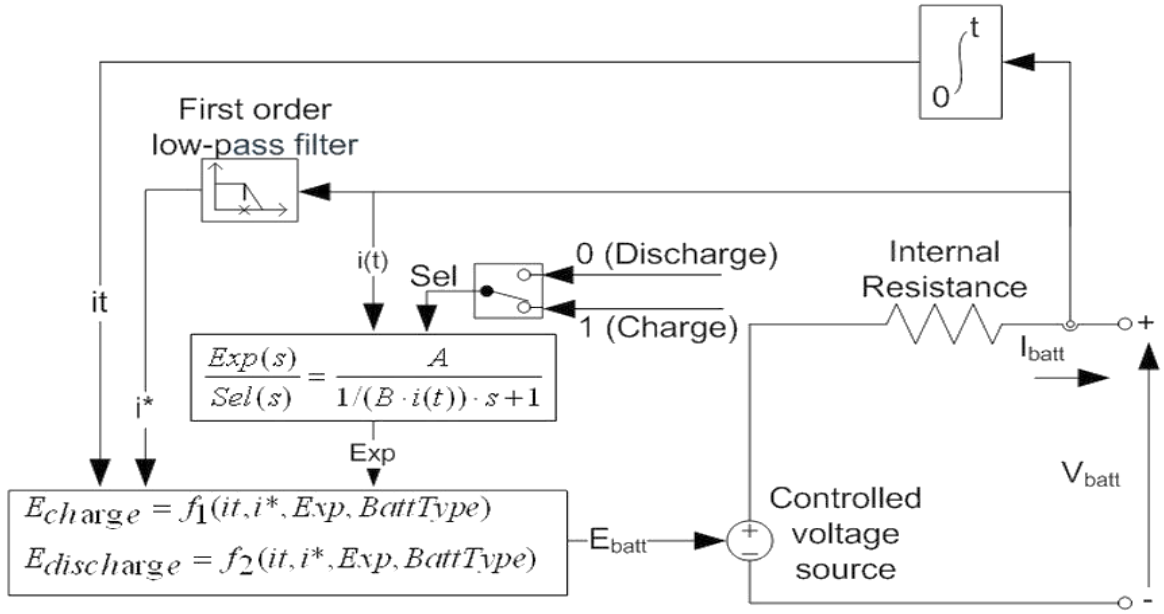

Fig. 5.1 Battery Equivalent Circuit of the Block Models

For the nickel-cadmium and nickel-metal-hydride battery types, the model uses these equations:

Discharge Model (i* > 0) $f_1(it, i*, i, Exp) = E_0 - K \cdot \frac{Q}{Q - it} \cdot i* - K \cdot \frac{Q}{Q - it} \cdot it + Laplace^{-1}\left(\frac{Exp(s)}{Sel(s)} \cdot 0\right)$

Charge Model (i* < 0) $f_2(it, i*, i, Exp) = E_0 - K \cdot \frac{Q}{|it| + 0.1 \cdot Q} \cdot i* - K \cdot \frac{Q}{Q - it} \cdot it + Laplace^{-1}\left(\frac{Exp(s)}{Sel(s)} \cdot \frac{1}{s}\right)$.

In the equations:

Here, E_{Batt} is nonlinear voltage, in V, E_0 is constant voltage, in V, Exp(s) is exponential zone dynamics, in V, Sel(s) represents the battery mode, Sel(s) = 0 during battery discharge, Sel(s) = 1 during battery charging, K is polarization constant, in Ah^{-1}, i* is low frequency current dynamics, in A, i is battery current, in A.

it is extracted capacity, in Ah. Q is maximum battery capacity, in Ah., A is exponential voltage, in V., B is exponential capacity, in Ah^{-1}.

6. CONTROL STRATEGY FOR MICROGRID

The ANN based control is quick, robust and stable. It has potential to improve the power quality and efficiency of the microgrid. The proposed control strategy is intended for the following two condition: change in the wind velocity, change in the solar irradiation. The block diagram of proposed ANN based control strategy for management of hybrid storage is shown in Fig. 6.1.

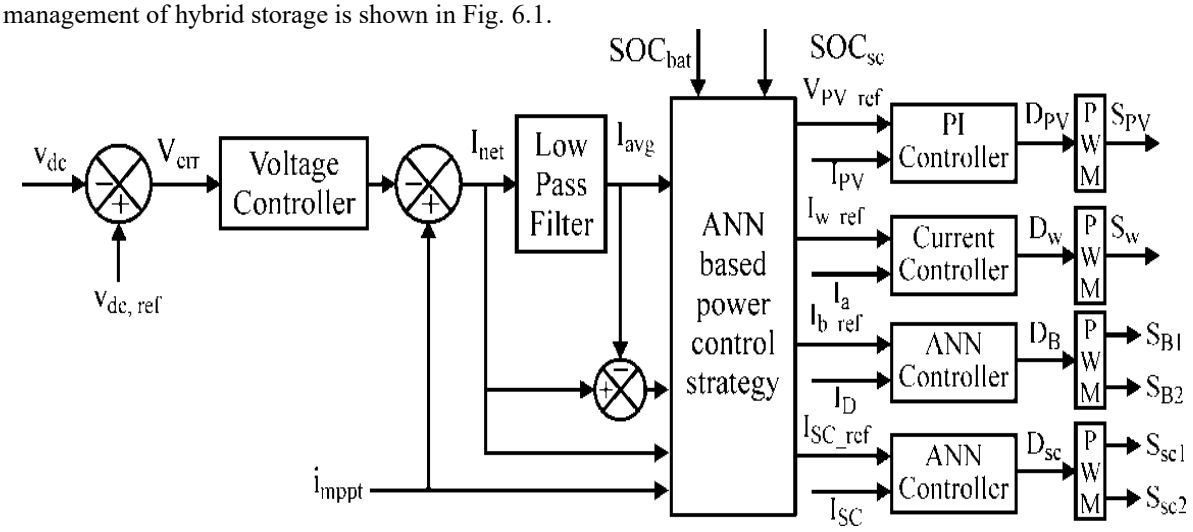

Fig. 6.1 Proposed ANN Based Control Strategy for Management of Hybrid Storage

7. SIMULATION RESULTS AND DISCUSSION

This system presents, following different Simulink studies designed to investigate the applications of the proposed control strategy with hybrid generation system in stand-alone power generation mode.

Case-1: Simulation Response during Asymmetrical (Line to Line) Fault at Constant Wind Speed (12 m/s) and Constant Load (8 kW) with Irradiance Changes (600W/m² to 800W/m², 800W/m² to 1000W/m²)

In this simulation test PV and WECS both works simultaneously. The irradiation of PV system varies from 600w/m^2 to 800w/m^2 and 800w/m^2 1000w/m^2 in stepped manner at constant temperature 25°C, while wind velocity and load kept constant at 12 m/s and 8kw respectively. The asymmetrical Line to line (L-L) fault is applied on phase A & B at the PCC bus for 1000 milliseconds time period. The simulation results obtained during the test are shown below. As shown in Fig 7 (a), the output voltage of the PV system is maintained constant, even fault is applied.

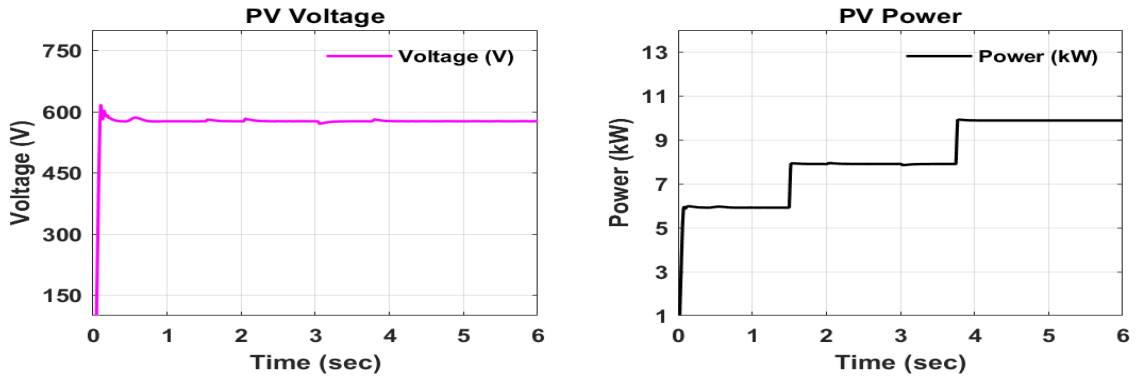

(a)

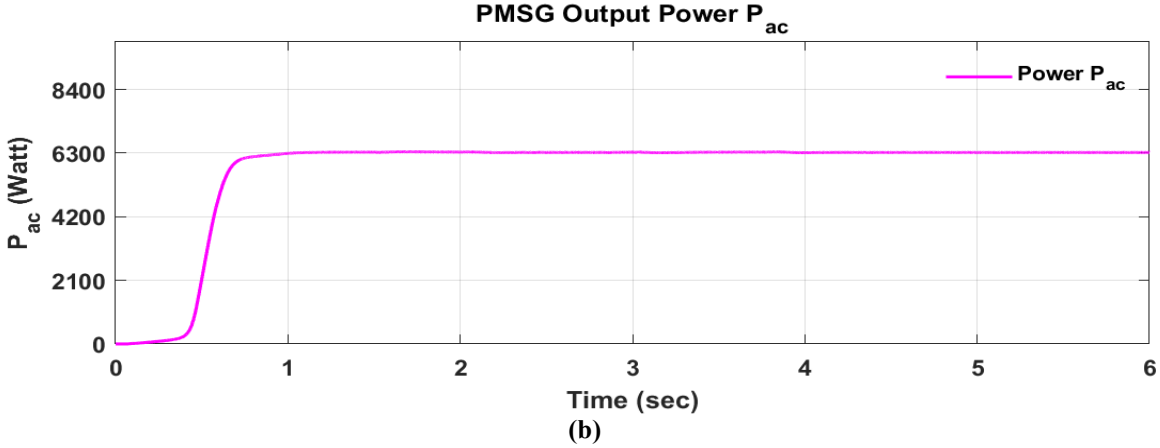

(b)

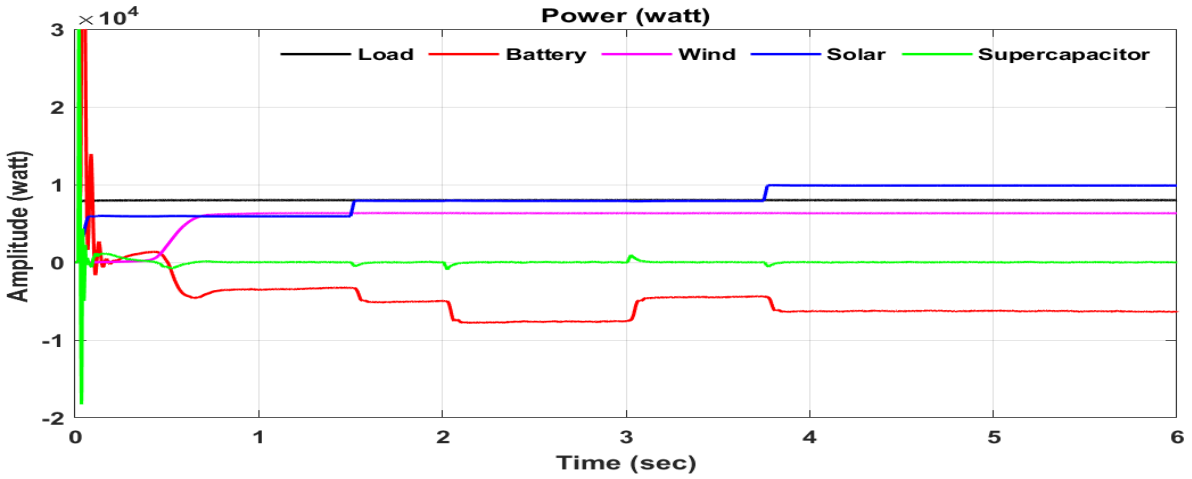

(c)

Fig. 7.1 Simulation Results of PV System & WECS during L-L Fault with Irradiance Change from 600W/m² to 800W/m², 800W/m² to 1000W/m², (a) PV Voltage (volt) and PV Output Power (kW), (b) PMSG Output Power P_{ac}, (c) Power Levels of Load, Battery, Wind, Solar System and Super capacitor

It is clear from Fig. 7.1 (a) that step increment in irradiation of the PV system from 600W/m² to 800W/m² at t = 1.5sec & 800W/m² to 1000W/m² at t = 3.75sec results in increment of PV output power 7.9kw and 9.8kw respectively. As the wind speed of the WECS is kept constant at 12m/s during the test, hence its output power is constant at 6.3kw throughout the test shown in Fig. 7.1(b). At t = 2sec the line to line (L-L) fault is applied at phase A, B. The output of the hybrid microgrid is not disturb during the fault interval t = 2sec to t = 3sec, that's prove that system works satisfactorily, even the fault is occurred. Power levels of load, battery, wind, solar system and supercapacitor are shown in Fig. 7.1 (c).

The simulation results of battery behavior during the L-L fault are shown in Fig. 7.2 (a) battery voltage and battery current and (b) battery SOC and battery reference current.

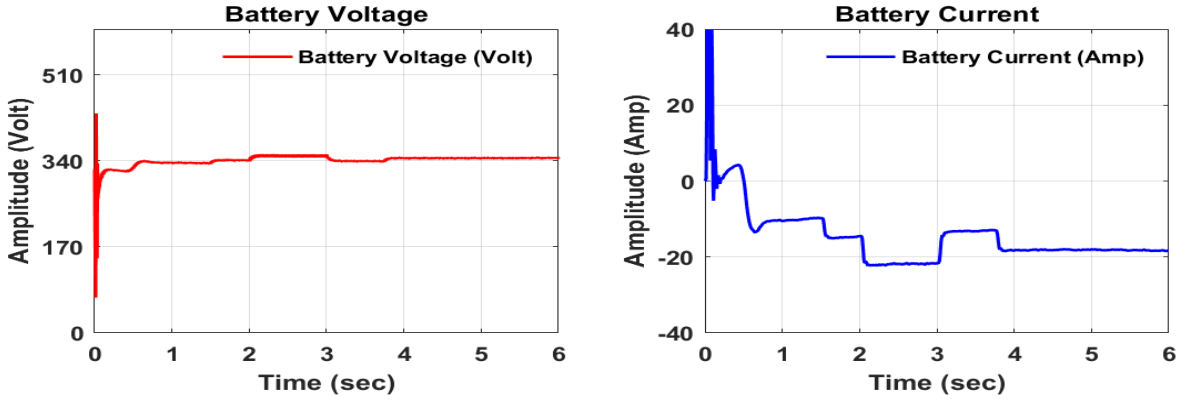

(a)

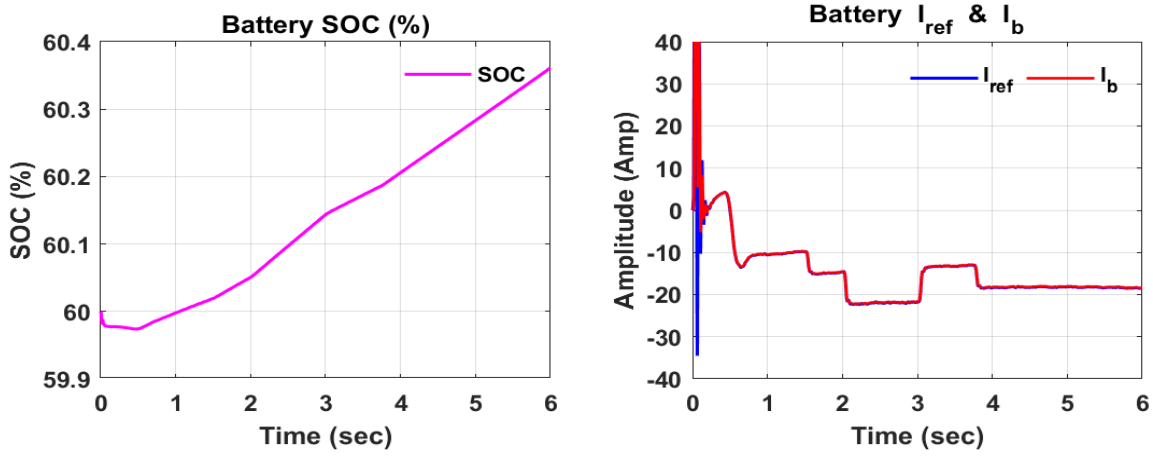

(b)

Fig. 7.2 Simulation Results of Battery behaviour During L-L fault, Waveform of (a) Battery Output Voltage (volt) and Battery Output Current (Amp), (b) Battery SOC (%) and Battery Reference Current

The Fig. 7.2 (a) shows that the battery voltage remains constant even during the L-L fault at 340V. Initially the SOC of the battery is set at 60%. At the starting of simulation between time period t = 0 to t = 1.5sec, the combined output of hybrid microgrid system is 12.2kw. The power output of the hybrid microgrid system is greater than the load demand and the battery system is in the charging mode with the charging current 10.5A. The SOC of the battery starts increasing from its initial value shown in Fig. 7.2 (b). At t = 1.5sec due to increment in irradiation of PV system, the combined output of hybrid microgrid system is increased to 14.2kw. The battery is keep charging with increased charging current i.e.,15A and the rate of rise of SOC is also increased. At time t = 2sec the line-to-line fault (LL) is applied at phase A & B at the PCC bus for 1000 milliseconds, during this period the complete hybrid system is isolated from the load side and the power generated by hybrid system is utilized to charge the battery and super capacitor. it is clear from Fig 7.2 (b), during the fault i.e., time interval t = 2sec to t = 3sec, the charging current of the battery is sharply increased to 22A and SOC of the battery linearly increased. The simulation results show that the developed control strategy effectively controls the power flow between microgrid generation and battery management system. At time t = 3.75sec, the combined output power of the hybrid microgrid is increased to 16.1kw, and battery charging current reached to 18.5A.

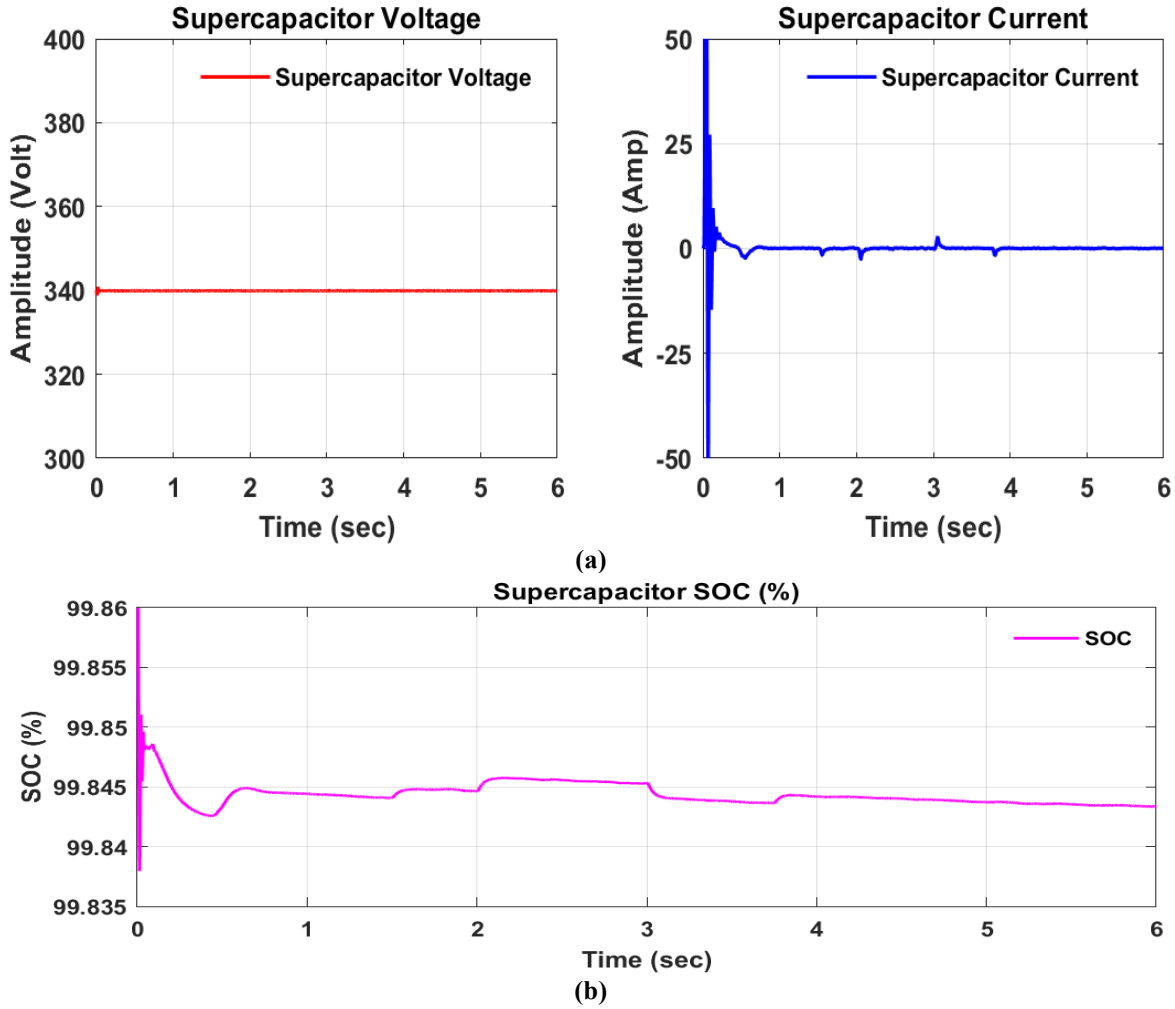

Fig. 7.3 Simulation Results of Super capacitor behavior during L-L Fault, Waveform of (a) Super capacitor Output Voltage (volt) and Super capacitor Output Current (Amp), (b) Super capacitor SOC (%)

The behavior of the super capacitor during L-L fault is shown in Fig 9. The super capacitor voltage maintained constant i.e., 340 V as shown in Fig 7.3 (a). In the developed novel control strategy, the assigned work to the super capacitor is to reduce the current stress to the battery by preventing it to cross the threshold value of current. As shown in Fig. 7.3 (a), when the irradiation changed from 600W/m^2 to 800W/m^2 at the time t = 1.5sec the super capacitor goes in to charging mode at that particular instant to reduce the current stress on the battery. The SOC of the super capacitor is increased as shown in Fig. 7.3 (b). At time t = 2sec when line-to-line fault (LL) is applied at the at the PCC bus for 1000 milliseconds, during this period the complete hybrid system is isolated from the load side and the power generated by hybrid system is utilized to charge the battery system. During the fault i.e., time interval t = 2sec to t = 3sec, the charging current of the battery is sharply increased, the super capacitor goes in to charging mode during fault interval to prevent the charging current of the battery to reach at threshold value, hence reduce the current stress of the battery as shown in Fig 7.3 (a) & (b).

During the test L-L fault is applied at the PCC bus between the time interval of t = 2 to 3sec. The source voltage at the PCC gets affected by line-to-line fault for the phase A & B. As seen from Fig. 10 the voltage of phase A & B reduce and phase C voltage is unaffected from the fault. During this fault interval the proposed DVR system injected the power to the faulty phase shown in Fig. 11 and keep the load voltage constant to the rated value and prevent the sensitive load to being affected by the voltage sag produced due to line to line fault at phase A & B, as shown in Fig. 7.4.

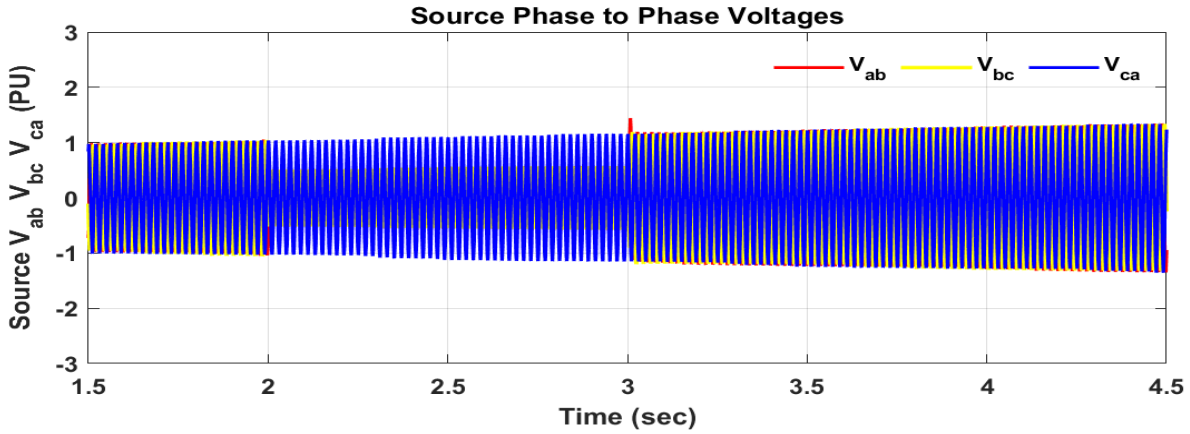

Fig. 7.4 Behavior of Source Voltage During L-L Fault

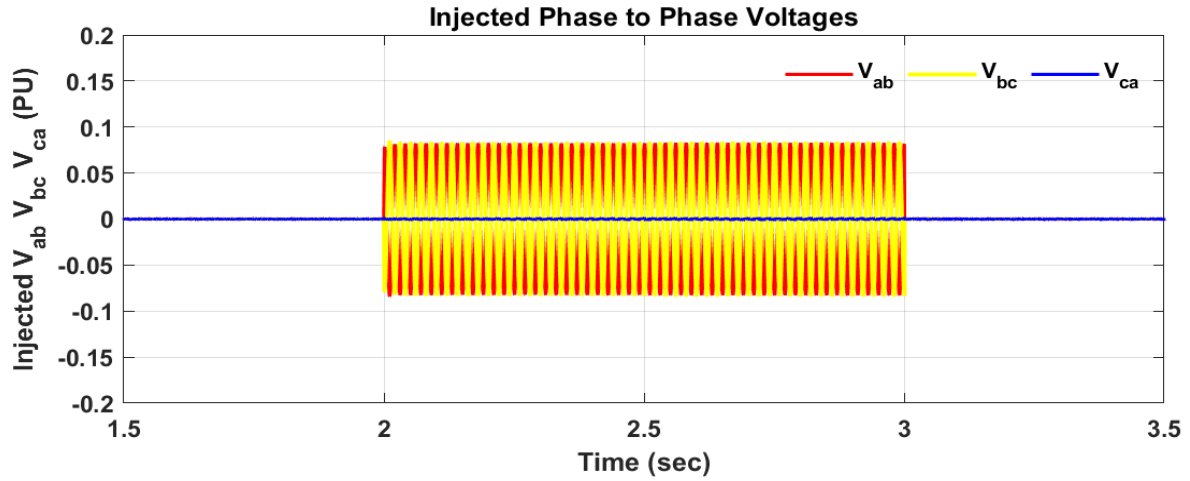

Fig. 7.5 DVR Injected Voltage at Phase A & B during L-L Fault

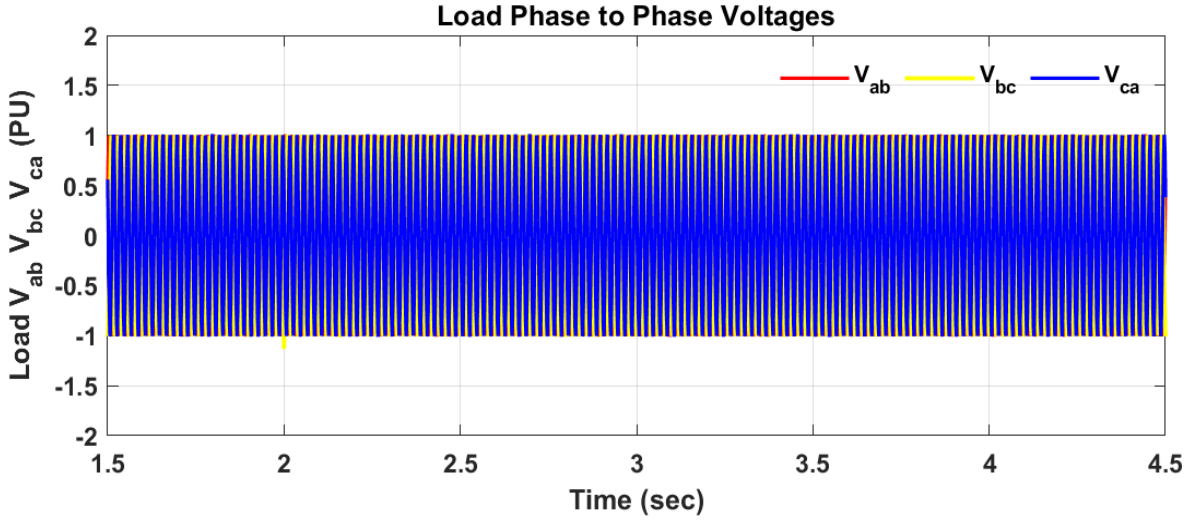

Fig. 7.6 Load Voltage during L-L Fault

CONCLUSION

In this paper, the main objective of this thesis is to improve the power quality of the hybrid microgrid system by solving the voltage sag and swell problem and reduce total harmonics distortion occurring due to various symmetrical and asymmetrical condition. The proposed system works in Artificial Neural network based novel

control strategy is proposed in this research work, which allows better voltage regulation at DC bus (±3.01V that fulfil the standards ± 5% range) compared to the conventional control strategy. ANN-based control of HESS quickly responds towards the change in the load and generation resulting in to smoothing of power with added advantage of increase in battery life span by reducing instantaneous current stress. The intelligent FLC based VSI inverter restrict the voltage output at desired level and reduce the harmonics distortion within the range specified by IEEE 519 standard.

REFERENCES

[1] Arul, P.G., Ramachandaramurthy, V.K. and Rajkumar, R. K., "Control strategies for a hybrid renewable energy system: A Review," Renewable and Sustainable Energy Reviews, vol. 42, pp. 597-608, 2015.

[2] Ahmed, S., Benoudjafer, C. and Benachaiba, C., "MPPT technique for standalone hybrid PV-Wind using fuzzy controller," In: Proceedings of Springer International conference on Artificial Intelligence in Renewable Energetic Systems held at Algeria during March 13-15, 2018, pp. 185-196, 2018.

[3] Alexander, A. and Thathan, M., "Modelling and analysis of modular multilevel converter for solar photovoltaic applications to improve power quality," IET Renewable Power Generation, vol. 9, pp. 78-88, 2015.

[4] Arezki, S. and Boudour, M., "Improvement of power quality for hybrid PV-FC power supply system," In: Proceedings of IEEE 16th International Power Electronics and Motion Control Conference and Exposition held at Turkey during September 21-24, 2014, pp. 725-730.

[5] Chauhan, A. and Saini, R.P., "A review on Integrated Renewable Energy System based power generation for stand-alone applications: Configurations, storage options, sizing methodologies and control," Renewable and Sustainable Energy Reviews, vol. 38, pp. 99-120, 2014.

[6] Chishti, F., Murshid. S and Singh, B. "LMMN based adaptive control for power quality improvement of grid intertie Wind-PV system," IEEE Transactions on Industrial Informatics, vol. 15, pp. 4900-4912, 2019.

[7] Chishti, F., Murshid. S and Singh, B., "Robust normalized mixed norm adaptive control scheme for PQ improvement at PCC of a remotely located Wind-Solar PV-BES Microgrid," IEEE Transactions on Industrial Informatics, vol. 16, pp. 1708-1721, 2019.

[8] Chishti, F., Murshid. S and Singh, B., "Weak grid intertie WEGS with hybrid generalized integrator for power quality improvement," IEEE Transactions on Industrial Electronics, vol. 67, pp. 1113-1123, 2020.

[9] Das, M. and Agarwal, V. 2015. "Novel high-performance stand-alone solar PV system with high gain, high efficiency DC-DC converter power stages," IEEE Transactions on Industry Applications, vol. 51, pp. 4718-4728, 2015.

[10] Faria, J., Pombo, J., Calado, M. and Mariano, S., "Power management control strategy based on artificial neural networks for standalone PV applications with a hybrid energy storage system," Energies, vol. 12, pp. 1-24, 2019.

[11] Frangieh, W. and Najjar, M. B., "Active control for power quality improvement in hybrid power systems," In: Proceedings of IEEE 3rd International Conference on Technological Advances in Electrical, Electronics and Computer Engineering held at Lebanon during April 29-30, 2015, pp. 218-223.

[12] Gayatri, M. T. L. and Parimi, A. M., "Power quality improvement of PV-WECS Microgrid using active power filter in real-time," In: Proceedings of IEEE 53rd International Universities Power Engineering Conference held at Glasgow, UK during September 4-7, 2018, pp. 1-6.

[13] Haruni, A. M. O., Negnevitsky, M., Haque, M. E. and Gargoom, A., "A novel operation and control strategy for a standalone hybrid renewable power system," IEEE Transactions on Sustainable Energy, vol. 4, pp. 402-4013, 2013.

[14] Houari, A., Djerioui, A., Saim, A., Ahmed, M. A. and Machmoum, M., "Improved control strategy for power quality enhancement in standalone systems based on four-leg voltage source inverters," IET Power Electronics, vol. 11, pp. 515-523, 2018.

[15] Hredzak, Agelidis, V. G. and Jang, M., "A Model predictive control system for a hybrid battery-ultracapacitor power source," IEEE Transactions on Power Electronics, vol. 29, pp. 1469-1479, 2014.

[16] Jayasankar, V. N. and Vinatha, U., "Implementation of adaptive fuzzy controller in a grid connected wind-solar hybrid energy system with power quality improvement features," In: Proceedings of IEEE Biennial International Conference on Power and Energy Systems: Towards Sustainable Energy held at Bengaluru during January 21-23, 2016, pp. 1-5.

[17] P. Kumar and V. Kumar, "Energy storage options for enhancing the reliability of Power system in the presence of Renewable Energy Sources," 2020 Second International Conference on Inventive Research in Computing Applications (ICIRCA), Coimbatore, India, 2020, pp. 1071-1076, doi: 10.1109/ICIRCA48905.2020.9183349.

[18] Kumar, P., Mathew, L., Shimi, S.L., Singh, P. (2016). Need of ICT for Sustainable Development of Power Sector. In: Satapathy, S., Joshi, A., Modi, N., Pathak, N. (eds) Proceedings of International Conference on ICT for Sustainable Development. Advances in Intelligent Systems and Computing, vol 408. Springer, Singapore. https://doi.org/10.1007/978-981-10-0129-1_63.

[19] Kumar, P., Kumar, V. (2022). Economic Analysis of Rural Distribution System with DER and Energy Storage System. In: Bansal, R.C., Zemmari, A., Sharma, K.G., Gajrani, J. (eds) Proceedings of International

Conference on Computational Intelligence and Emerging Power System. Algorithms for Intelligent Systems. Springer, Singapore. https://doi.org/10.1007/978-981-16-4103-9_20.

[20] Kerem, A., Aksoz, A., Saygin, A. and Yilmaz, E. N., "Smart grid integration of micro hybrid power system using 6-switched 3-level inverter," In: Proceedings of IEEE 5th International Istanbul Smart Grid and Cities Congress and Fair (ICSG) held at Turkey during April 19-21, 2017, pp. 161-165.

[21] Kim, J. S., Kwon, J. M. and Kwon, B. H., "High-efficiency two-stage three-level grid-connected photovoltaic inverter," IEEE Transactions on Industrial Electronics, vol. 65, pp. 2368-2377, 2018.

[22] Kotra, S. and Mishra, M. K., "A supervisory power management system for a hybrid microgrid with HESS," IEEE Transactions on Industrial Electronics, vol. 64, pp. 3640-3649, 2017.

[23] Lazarov, V., Notton, G., Zarkov, Z. and Bochev, I., "Hybrid power systems with renewable energy sources types, structures, trends for research and development," In: Proceedings of 11th International conference on electrical machines, drives and power systems, held at Bulgaria during September 15-16, 2005, pp.515-520.

[24] Lei, M., Yang, Z., Wang, Y., and Honghua, X., "Design of energy storage control strategy to improve the PV system power quality," In: Proceedings of IEEE 42nd Annual Conference of the Industrial Electronics Society (IECON) held at Italy during October 23-26, 2016, pp. 2022-2027.